J. Fluid Mech. (1989), *vol.* 200, *pp.* 367–387
Printed in Great Britain

The relaxation of a turbulent boundary layer in an adverse pressure gradient

By ANDREW D. CUTLER† AND JAMES P. JOHNSTON‡

†The George Washington University JIAFS, NASA Langley Research Center, Hampton, VA 23665, USA

‡Department of Mechanical Engineering, Stanford University, Stanford, CA 94305, USA

(Received 9 July 1985 and in revised form 19 September 1988)

The relaxation of a reattached turbulent boundary layer downstream of a wall fence has been investigated. The boundary layer has an adverse pressure gradient imposed upon it which is adjusted in an attempt to bring the boundary layer into equilibrium. This is done by adjusting the pressure gradient so as to bring the Clauser parameter (G) down to a value of about 11.4 and then maintain it constant. In the region from the reattachment point to 2 or 3 reattachment lengths downstream, the boundary layer recovers from the initial major effects of reattachment. Farther downstream (where G is constant) the pressure-gradient parameter changes very slowly and profiles of non-dimensionalized eddy viscosity appear self-similar. However, pressure gradient and eddy viscosity are both roughly twice as large as expected on the basis of previous studies of equilibrium turbulent boundary layers. It is not known whether equilibrium has been achieved in this downstream region. This is another illustration of the great sensitivity of boundary-layer structure to perturbations.

1. Introduction

This is a study of two-dimensional turbulent boundary layers relaxing downstream of separation and reattachment in cases where the shear layer at reattachment is much thicker then the boundary layer upstream of separation. The relaxation of the boundary layer downstream of reattachment is a slow process which cannot be predicted accurately using current turbulence models. Depending on the surface geometry and the nature of the device that produces the separation, a streamwise distance of more than 100 times the shear-layer thickness at reattachment may be required before the boundary layer regains an equilibrium structure. Boundary layers downstream of reattachment are of practical importance, for example downstream of a shock-induced separation on a supercritical aerofoil, or downstream of a step or discontinuity on a flow surface. Previous experimental investigations of the relaxation of a reattached boundary layers have only considered relaxation in a zero pressure gradient, but in many cases of practical importance relaxation occurs in an adverse pressure gradient. In fact the behaviour of boundary layers is most critical in those flow devices for which the pressure gradient is adverse, for example diffusers and aerofoils, since their limiting performance is determined by boundary-layer growth and separation.

Flow separation and reattachment has been reviewed recently by Simpson (1985), and Bradshaw & Wong (1972) contains a review of reattachment and relaxation downstream of a variety of surface discontinuities, including fences and backsteps. We know of no previous studies of the effect of adverse pressure gradient on the

relaxation of the boundary layer downstream of reattachment, although Driver & Seegmiller (1985) have studied reattachment in diverging channel flows. Most of the detailed studies of reattachment have been backward-facing steps (backsteps) which have the advantage of simple geometry and a single, well-defined separation point. Fences with a variety of geometries are also commonly used because of their practical importance and the ease with which they can be mounted on the wall of a wind-tunnel test section.

We shall present the results of an experimental study of a turbulent boundary layer flowing in an adverse pressure gradient downstream of a wall fence. Extensive mean flow and turbulence measurements have been made from reattachment until the boundary layer begins to merge with the opposite wall boundary layer far downstream. No detailed measurements have been made in the region of separated flow because of the difficulties in using hot wires in this region, although the reattachment length has been estimated. Sufficient information is available to aid development of, or to verify, methods for calculating boundary layers downstream of reattachment.

We chose in our experiment to investigate the relaxation of a reattached boundary layer towards an equilibrium form. An equilibrium boundary layer is one in which boundary conditions and pressure gradient expressed in an appropriate non-dimensional form are held constant, and the boundary layer has developed until properly non-dimensionalized profiles of mean velocity become self-preserving. Self-preserving laminar boundary layers exist, but properly self-preserving turbulent boundary layers do not. However turbulent boundary layers that are self-preserving in the outer layer, apart from a small effect of Reynolds number, are possible and these we call equilibrium turbulent boundary layers. They have been investigated by many authors, including Clauser (1954, 1956), Townsend (1960, 1976), Bradshaw (1967) and East & Sawyer (1979). The test-section geometry in our experiment, and consequently the pressure gradient downstream of reattachment, was adjusted in a manner similar to that used by Clauser (1954) so that the Clauser mean velocity profile shape factor G fell to a predetermined value and then, downstream of this point, was maintained constant.

2. Experimental method

The low-turbulence closed-return wind tunnel described by Cutler (1984) was used for this experiment. The wind tunnel includes a heat exchanger to maintain the air temperature nearly constant and a secondary blower to make up air discharged through slots to the atmosphere at the test section. The test section is shown in figure 1. It consists of a parallel-walled (305 mm wide $\times$ 102 mm high) inlet duct followed by a diffuser and is preceded by a 6:1 flow contraction. One wall of the test section, designated the test wall, is flat throughout and is the wall on which the boundary layer of interest flows. The test-wall boundary layer is tripped to produce transition to turbulence by a 0.79 mm high $\times$ 6.35 mm wide rectangular section trip located 64 mm after the end of the contraction, and then it separates at a 7.37 mm high by 6.35 mm wide rectangular-section wall-mounted fence located 187 mm from the exit of the contraction. In fact, the boundary layer separates just ahead of the fence, then reattaches and separates again at the leading corner of the fence, before reattaching on the test wall further downstream; the flow does not reattach to the fence downstream of the leading corner (Castro 1981). The boundary layer 99% thickness (δ_{99}) just ahead of the fence is 4.8 ± 0.5 mm ($0.65h$). Castro & Fackrell (1978), in an

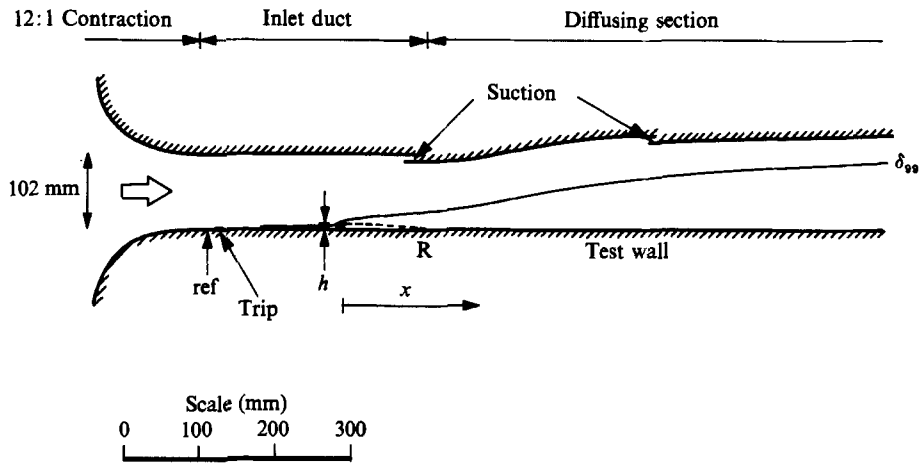

FIGURE 1. Test section (flow is from left to right); ref is the reference station for C_p, h is the fence height (7.37 mm), x is the streamwise coordinate, R is the reattachment point.

experiment where the boundary-layer thickness ahead of a wall-mounted fence of small thickness was varied, showed that for $\delta_{99}/h < 0.6$ there was no perceptible effect of this parameter on the flow downstream of the fence, and for δ_{99}/h as high as 1.0 the effect was only a 5% reduction in reattachment length.

The boundary layer reattaches in the inlet duct before entering the diffusing section, the diffusing section being located sufficiently far downstream of reattachment that the separated-flow region and reattachment are not significantly effected by its presence. The reattachment length (x_r), the distance from the *downstream* face of the fence to reattachment (the point of zero wall shear stress), is an important parameter which is commonly used in non-dimensionalizing the streamwise (x) coordinate. It was not measured directly in this experiment, but was estimated to be 115 ± 5 mm by fitting the wall pressure distribution close to reattachment to data from a wide range of reattaching flows for which x_r was measured, including fence flows. The normalization first proposed by Roshko & Lau (but see Westphal & Johnston 1983, figure 6.2), which collapses the pressure distribution onto a universal curve within $-0.6x_r$ and $0.2x_r$ of reattachment, was used in the fitting.

The wall opposite the test wall in the diffusing section is flexible and its geometry may be adjusted to produce different adverse pressure gradients. Slots in this wall and the two endwalls provide a boundary-layer bleed ensuring that no separation occurs in the diffusing section.

Spanwise profiles of the total pressure in the inlet-duct free stream show a peak-to-peak variation of less than 0.4% (0.2% in the velocity) and free stream $(\overline{u^2})^{\frac{1}{2}}/U$ levels are less than 0.2%. Spanwise profiles of the total pressure in the test-wall boundary layer, which were obtained in the inlet duct with the fence absent, also show good two-dimensionality, with peak-to-peak variation in local dynamic pressure less than 8% (4% in velocity) in the central 90% of the span.

A momentum-integral balance was appled to the test-wall boundary layer (the PL–PR balance, see Coles & Hirst 1968) downstream of the wall fence to verify the two-dimensionality and the accuracy of the mean flow data. The maximum discrepancy between PL and PR in the range $x = 122$ mm to $x = 618$ mm was no

more than 5% of $U_e^2\theta$ measured at the first station ($x = 122$ mm), which indicates that the flow is two-dimensional to within the expected uncertainty of PL and PR. Some caution should be used in interpreting the results far downstream since, at the last profile station ($x = 618$ mm), the test-wall boundary-layer thickness δ_{99} has grown to nearly 70% of the diffuser height and nearly 30% of the diffuser width. However, the test-wall boundary layer does not begin to merge with the opposite wall boundary layer until downstream of this point since the opposite wall boundary layer is thin as a consequence of the boundary-layer bleed. The ratio of δ_{99} to width of nearly 30% exceeds a little the limit specifed by de Brederode & Bradshaw (1978) of 25% for the effect of a sidewall boundary layer to be neglected. However, as a consequence of boundary-layer bleed and a lower growth rate, the slightly diverging sidewall boundary laycrs are thinner than the reattached test-wall boundary layer, so that the ratio of sidewall boundary-layer thickness to diffuser width is significantly less than de Brederode & Bradshaw's limit.

Measurements of total pressure were made by using a Pitot probe with a tip constructed of 0.62 mm diameter, circular-section hypodermic needle ground square at the end. Mean velocity and turbulence statistics were obtained with hot-wire anemometers. A normal hot wire (DISA 55-P15) was used for measuring mean and fluctuating u, and an $\times$-wire (DISA 55-P51) for mean and fluctuating u and v. The wires were DISA 5 micron platinum-plated tungsten wires, gold plated at the ends, and the hot-wire bridge was a TSI model 1050. Closely spaced static pressure taps gave the wall pressure distribution. Air temperature was monitored during data acquisition using an Omega (44034) thermistor. The data acquisition and experiment control was by a DEC MINC microcomputer and the $\times$-wire data acquisition and much of the post-processing was by a DEC VAX 11-750. Traverses were with a computer-controlled, stepping-motor operated traversing mechanism and static pressure data acquisition was with a Scanivalve system. Hot wires were calibrated by fitting to a King's law, $e^2 = a + bU^n$, where a, b and n were optimized and angular calibration of $\times$-wires was by yawing the probe as suggested by Bradshaw (1971). Linearization and processing to obtain turbulence statistics was performed digitally and in real time using the micro computer or the VAX. Small corrections were made to the hot-wire results for any small drift in temperature which did occur during a run.

Small corrections were applied to the normal hot-wire data (subscript c) to account for the effects of high turbulence intensity and any small inclination of the mean flow streamlines with respect to the wall by using the following formula:

$$U_c = U(1-e_1), \quad \overline{u_c^2} = \overline{u^2}(1-e_2),$$

where

$$e_1 = \frac{V^2+\overline{v^2}}{2U^2}, \quad e_2 = \frac{2\overline{uv}V+\overline{uv^2}}{\overline{u^2}U}.$$

These formulae were derived following Bradshaw (1971) and the quantities in the terms e_1 and e_2 were all interpolated from $\times$-wire measurements at the same streamwise location. Data were rejected at locations where flow reversals occurred more than 5% of the time – in practice normal wire data were rejected where $(\overline{u^2})^{\frac{1}{2}}/U > \frac{1}{2}$ and $\times$-wire data were rejected where $(\overline{u^2}+\overline{v^2})^{\frac{1}{2}}/U > 1/(2\sqrt{2})$. Agreement between profiles of U and $\overline{u^2}$ measured with the normal wire (corrected) and the $\times$-wire is well within the uncertainties quoted in table 1. The $\times$-wire technique was validated in the fully developed turbulent channel flow described

Probe type	Quantity	Uncertainty
Static tap	C_p	± 0.01
Normal hot wire	U	$\pm 0.015U$
	$\overline{u^2}$	$\pm 0.04\overline{u^2}$
Crossed hot wire	U	$\pm 0.015U$
	$\overline{u^2}$	$\pm 0.06\overline{u^2}$
	$\overline{v^2}$	$\pm 0.15\overline{v^2}$
	$\overline{uv}$	$\pm 0.09\overline{uv}$

TABLE 1. Estimated uncertainty in directly measured quantities. All uncertainties are quoted at 20:1 odds.

by Hussain & Reynolds (1975) in which the shear stress can be derived from measurements of streamwise pressure gradient.

The boundary-layer edge thickness, δ_{99}, was obtained as the point where the mean velocity, deduced from Pitot measurements of total pressure and the wall static pressure, reached 99% of the free-stream value. Mean velocity profiles from the normal hot wire were integrated to obtain the boundary-layer integral thicknesses. The definitions of East (1981), which account for any small effect of flow curvature, were used:

$$\delta^* = \int_0^\infty (U_p - U)\,\mathrm{d}y/U_{pw},$$

$$\theta = \int_0^\infty ((U_p^2 - U^2) - U_{pw}(U_p - U))\,\mathrm{d}y/U_{pw}^2.$$

Here, U_p is the velocity calculated from the free-stream total pressure and the static pressure at the given y-location. It can easily be obtained at the wall (denoted U_{pw}) where there are static pressure taps, and in the free stream it is simply the mean velocity. Since U_{pw} and U_e, the value of U_p at δ_{99}, differ by no more than 1.5% in this experiment, it was considered acceptable to obtain U_p at intermediate points using a simple interpolation scheme. The skin-friction coefficient, $C_f = \tau_w(\frac{1}{2}\rho U_{pw}^2)$, was estimated from normal hot-wire mean velocity profiles by fitting to the logarithmic law of the wall in the range $50 < y^+ < 110$, where $u^+ = U/u_\tau$ and $y^+ = yu_\tau/\nu$:

$$u^+ = (1/0.41)\ln y^+ + 5.0.$$

Skin friction was also estimated using the Ludweig–Tillman (L–T) correlation (see White 1974):

$$C_f = 0.246 Re_\theta^{-0.268}\, 10^{-0.678H}.$$

Agreement in C_f between these two methods is within $\pm 5\%$. The results discussed below were obtained with the law-of-the-wall fit, and have an uncertainty of less than $\pm 10\%$.

Air temperature varied less than ± 0.2 °C for the acquisition of any given profile of data, and the temperatures for all data sets are within one or two degrees of each other. The kinematic viscosity was $15.50 \pm 0.05 \times 10^{-6}$ m^2/s.

Parameters of the mean flow are given in table 2. The full data set, including mean velocities U and V, the Reynolds stresses, $\overline{u^2}$, $\overline{uv}$, $\overline{v^2}$, the triple products $\overline{u^3}$, $\overline{u^2v}$, $\overline{uv^2}$, $\overline{v^3}$ and the fourth-order statistics $\overline{u^4}$, $\overline{v^4}$, is tabulated in Cutler (1984) where it is

x (mm)	δ_{99} (mm)	δ^* (mm)	θ (mm)	G	C_f log law	C_f L–T	U_e (m/s)	U_{pw} (m/s)	dU_{pw}/dx (1/s)
120 (122)	26.2	9.43	4.41	—	—	0.00070	42.4	42.5	−38.4
158 (160)	29.9	7.66	4.66	14.4	0.00149	0.00151	41.1	40.8	−8.3
196 (198)	34.9	7.76	5.16	10.9	0.00189	0.00184	40.2	40.1	−29.6
234 (236)	41.5	8.97	6.10	10.5	0.00186	0.00187	38.6	38.7	−41.3
272 (274)	49.1	9.93	6.76	10.7	0.00178	0.00184	36.9	37.1	−38.8
310 (312)	55.1	11.70	7.85	11.4	0.00166	0.00173	35.2	35.7	−31.1
387 (389)	64.5	14.00	9.37	11.6	0.00163	0.00165	33.7	34.0	−16.0
463 (465)	70.8	15.40	10.30	11.4	0.00167	0.00164	32.9	33.0	−11.0
539 (541)	77.2	16.60	11.20	11.2	0.00168	0.00163	32.1	32.2	−9.0
615 (617)	81.8	17.70	11.90	11.2	0.00170	0.00161	31.5	31.6	−8.3

TABLE 2. Parameters of the mean flow. The number in brackets in the first column refers to the location of δ_{99}, which has been obtained from Pitot data.

designated Case 'C'. Detailed hot-wire measurements are only given downstream of reattachment, but the information is sufficient for developing and verifying computer methods for calculating reattached boundary layers. The following Section discusses in more detail the mean flow and turbulence results.

3. Results

The results for the skin-friction coefficient and the Clauser parameter (defined $G = (H-1)/(HC_f^{\frac{1}{2}}/2)$, where $H = \delta^*/\theta$) are given in table 2. The skin-friction coefficient initially rises rapidly before falling again more slowly, and the Clauser parameter initially falls rapidly before attaining a nearly constant value around 11.4. Figure 2 shows the development of the wall static pressure coefficient, defined as

$$C_p = (p - p_{\text{ref}})/(\tfrac{1}{2}\rho U_{\text{ref}}^2);$$

the reference pressure (p_{ref}) and reference velocity ($U_{\text{ref}} = 39.14$ m/s) are measured at $x = -181$ mm (marked 'ref' in figure 1). Also shown in figure 2 is the gradient of C_p, obtained by locally fitting the C_p data in a centred manner to a fourth-order polynomial, and differentiating. The pressure coefficient in the region from $x = 50$ mm to $x = 100$ mm (the region of separated flow) is large and negative and the pressure coefficient gradient is also very large – both are out of range in the figure. In the diffusing section the pressure gradient initially rises rapidly but then falls slowly as the pressure gradient needed to maintain constant G falls.

The fact that G is maintained constant does not necessarily mean that the boundary layer is equilibrium. The boundary-layer edge velocity U_e must also vary as a power law of the form $U_e = C(x-x_0)^a$, where x_0 is an effective origin and C a constant (Townsend 1976). The exponent in this power law ranges from positive values which correspond to a favourable pressure gradient, to negative values as large as -0.25 or -0.30 (depending on Reynolds number) which correspond to an adverse pressure gradient. Development of lengthscales such as the boundary-layer thickness and the mixing length will then be linear and of the form $l = l_0(x-x_0)$. The boundary-layer thickness parameters δ_{99}, δ^*, and θ in our experiment have been fitted to straight lines in the region $x = 463$–615 mm to give the location of the apparent origin, $x_0 = -411$ mm; both the fits and the data are shown in figure 3. The constant C and exponent a in the power law were then determined from a least-

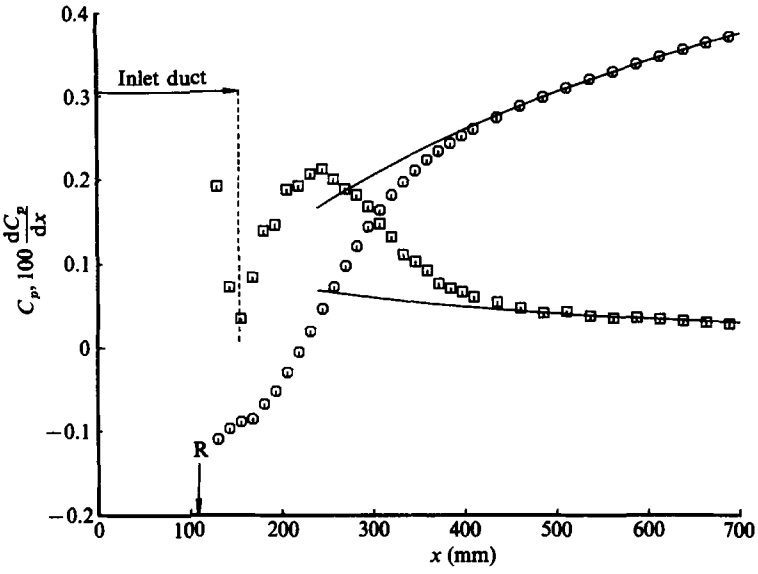

FIGURE 2. Development of the pressure coefficient C_p (○), 100 times the gradient dC_p/dx in mm^{-1} (□), and C_p and its gradient given by the power law $U_{pw}/U_{ref} = 2.818(x+411)^{-0.27}$(——).

squares fit to the C_p data to obtain the following expression (where x is measured in mm):

$$U_e/U_{ref} = 2.818(x+411)^{-0.27}.$$

This expression has been converted to an expression for C_p and one for dC_p/dx which are compared to the experimental data in figure 2. These expressions are a good fit to the data downstream of $x = 400$ or 450 mm in the region where G is roughly constant, suggesting that the boundary layer is in equilibrium in this region. However, the exponent (-0.27) is larger in magnitude than -0.22, the value interpolated from the results of previous studies of equilibrium turbulent boundary layers for $G = 11.4$ (Bradshaw 1967).

A practically equivalent definition of an equilibrium turbulent boundary layer requires that, instead of a power-law variation of U_e, the Clauser pressure gradient parameter, $\beta = \delta^*/\tau_w\, dp/dx$, is maintained constant (Clauser 1954). In figure 4 we have plotted G as a function of β and some results from the literature for equilibrium turbulent boundary layers. At the three downstream stations, from $x = 463$ to 615 mm, β takes a nearly constant value roughly twice that suggested by the curve fit of Nash (1965). Thus in terms of all mean flow parameters a state of equilibrium would appear to have been achieved by $x = 400$ or 450 mm, but the values of a and β do not correspond to those expected on the basis of previous studies for $G = 11.4$.

In order to show the development of the total pressure along mean streamlines we have plotted in figure 5 the defect of total pressure coefficient, $(P_e - P)/(\frac{1}{2}\rho U_{ref}^2)$, as a function of the stream function,

$$\psi = \int_0^y U/U_{ref}\, dy.$$

The total pressure is seen to rise close to the wall and fall farther out in a smooth and monotonic fashion, with the rate of change near the wall comparable with that farther out. This is in contrast to typical zero-pressure-gradient boundary layers

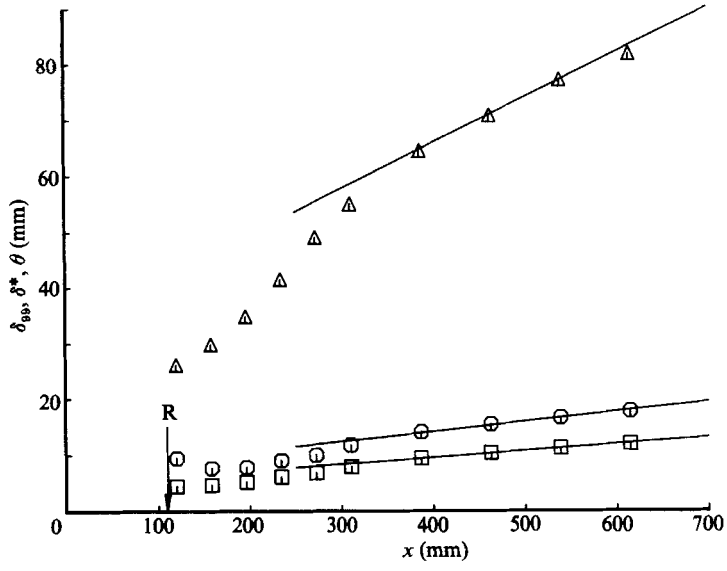

FIGURE 3. Development of the boundary-layer thickness parameters, δ_{99} (△), δ^*, (○), and θ (□). Also, linear developments with the origin at $x = -411$ mm.

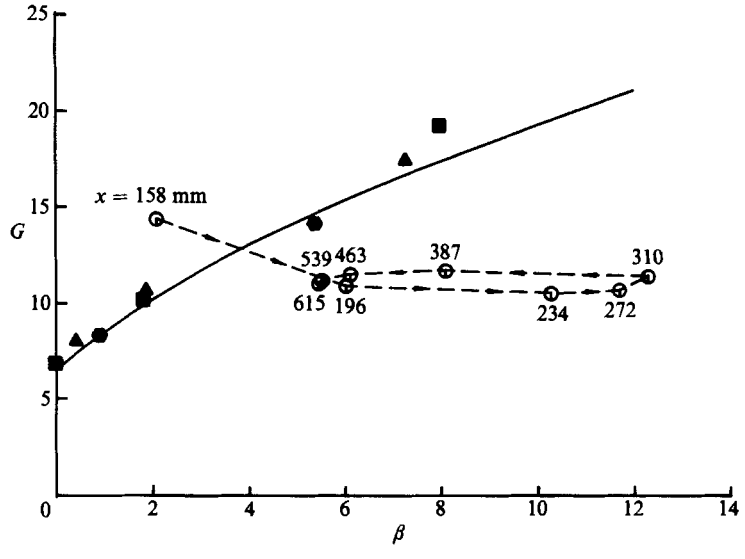

FIGURE 4. Development of the Clauser shape parameter as a function of the pressure gradient parameter β (○); Nash (1965) fit to equilibrium data, $G = 6.1(\beta+1.81)^{\frac{1}{2}}-1.7$ (——); equilibrium data due to Clauser (1954) (■); Bradshaw (1967) (●); and East & Sawyer (1979) (▲).

where the flow near the wall tends to respond much more quickly to imposed changes in boundary conditions such as surface roughness and pressure gradient (Smits & Wood 1985).

Several profiles of the mean U-component velocity measured with normal hot wires are plotted in wall coordinates (u_τ is obtained by fitting to the logarithmic law) in figure 6. All profiles have extensive logarithmic regions and the profiles can be fitted by the law of the wall and the wake (Coles in Coles & Hirst 1968). Profiles of the

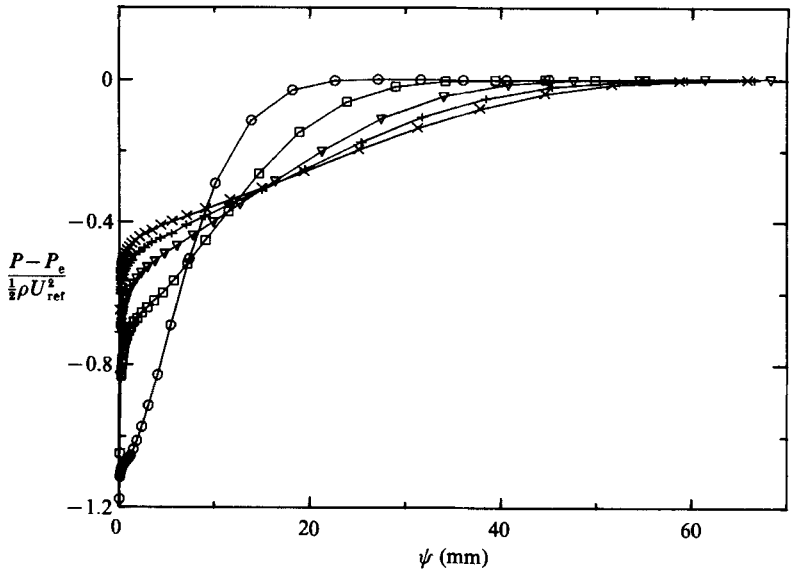

FIGURE 5. Profiles of the defect of total pressure coefficient, as a function of the stream function. The profiles are at $x = 122$ mm (⊙), 198 mm (⊡), 312 mm (▽), 465 mm (+), and 617 mm (×).

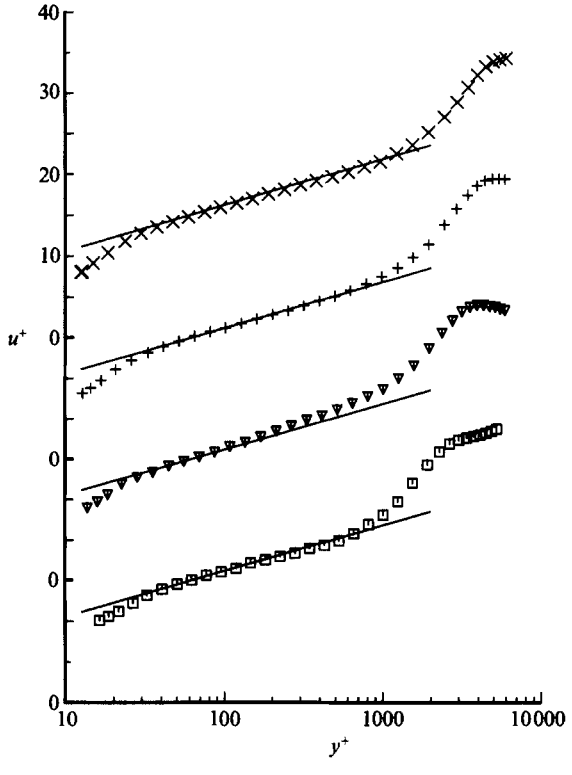

FIGURE 6. Profiles of mean U-component velocity in wall coordinates at $x = 196$ mm (□), 310 mm (▽), 463 mm (+), and 615 mm (×). For comparison $u^+ = (1/0.41)\ln(y^+) + 5.0$ (——).

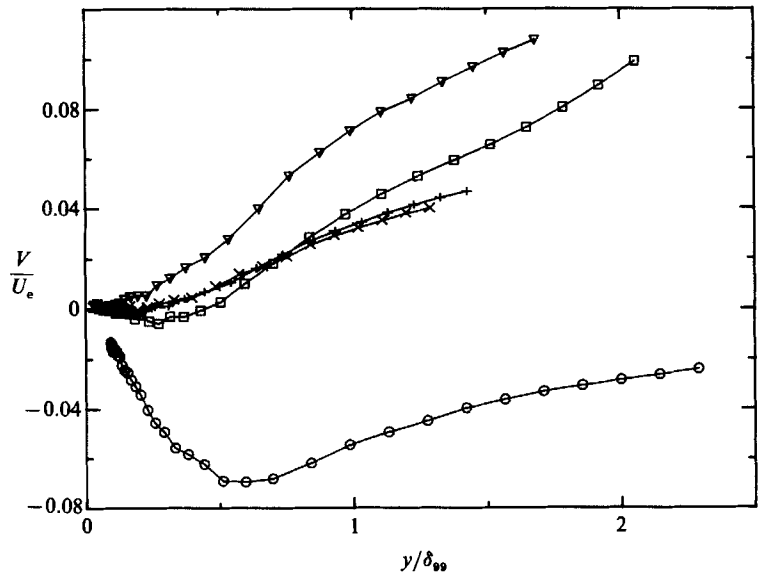

FIGURE 7. Profiles of mean V-component velocity. The profiles are at $x = 122$ mm (⊙), 199 mm (⊡), 313 mm (▽), 465 mm (+), and 618 mm (×).

V-component velocity obtained with the × -wire are plotted in figure 7 and show that near reattachment there is a region with significant mean streamline concave curvature within the boundary layer, but that farther downstream the streamlines are nearly straight. In the region of concave curvature, δ_{99}/R is roughly 0.04 (R is the radius of curvature of the mean flow streamlines at the edge of the boundary layer). Barlow & Johnston (1985) show that noticeable structural changes take more than 10° and 20° of turning to develop in a boundary layer on a concavely curved surface with $\delta_{99}/R = 0.06$–0.08, and since no more than about 7° of turning occurs in our experiment it is unlikely that significant structural changes occur as a result.

The Reynolds stresses, shown in figure 8, peak near the centre of the boundary layer, a feature of both the free shear layer ahead of reattachment and of typical adverse-pressure-gradient boundary layers. The peak Reynolds stresses fall monotonically in the downstream direction but the shapes of the profiles change little. For the sake of brevity the triple products ($\overline{u^3}$, $\overline{u^2v}$, $\overline{uv^2}$, $\overline{v^3}$) are not shown here, but these behave in a similar manner to the Reynolds stresses, with high levels near reattachment which fall monotonically in the downstream direction.

4. Derived results and modelling

If mean streamline angles with respect to the wall are large in a boundary layer and the streamlines are nearly straight, then it may be appropriate to model the turbulent stresses in a streamline coordinate system in which x_s is tangential to the mean streamline direction at each point in the flow, $z_s = z$ (unchanged) and y_s is normal to x_s and z_s, rather than in the wall system in which the data is measured. The shear stress in the streamline coordinate system may be obtained by using the following expression:

$$-\overline{u_s v_s} = -\overline{uv}\cos(2\alpha) + \tfrac{1}{2}(\overline{u^2} - \overline{v^2})\sin(2\alpha),$$

where $\tan(\alpha) = V/U$. In separating turbulent boundary layers, where typically

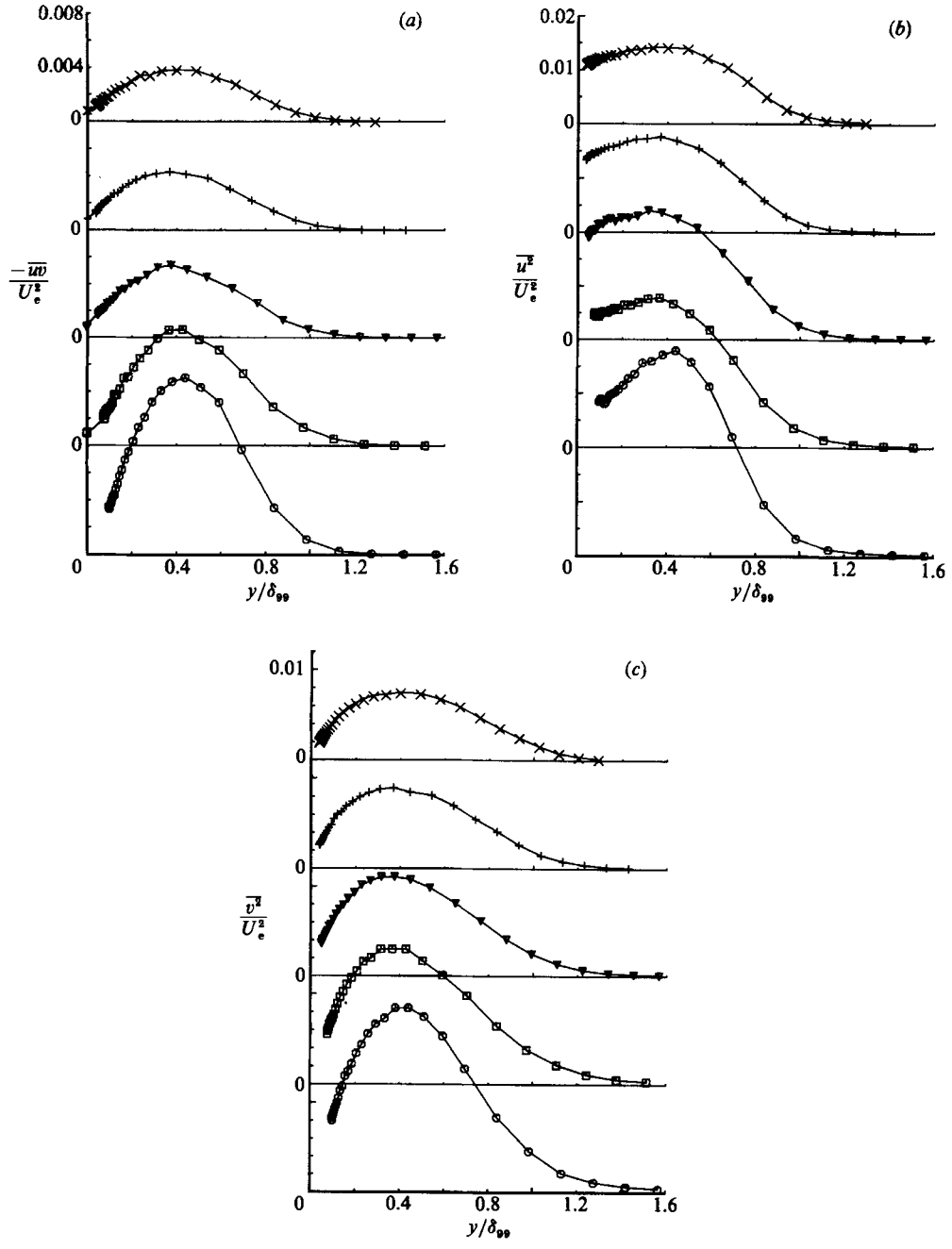

FIGURE 8. (*a*) Profiles of turbulent shear stress, $-\overline{uv}/U_e^2$. Wall points are $\frac{1}{2}C_f$ from a fit of mean velocity to the log law. (*b*) Profiles of $\overline{u^2}/U_e^2$. (*c*) Profiles of $\overline{v^2}/U_e^2$. For the profile locations, see figure 7.

$\alpha = 5°$–$15°$ and $-\overline{uv}$ and $-\overline{u_s v_s}$ can differ by more than 50%, some of the conventional models for $-\overline{uv}$, such as the structural parameter ($a_1 = -\overline{uv}/(\overline{u^2}+\overline{v^2}+\overline{w^2})$, more accurately represent the data when $-\overline{u_s v_s}$ is used instead (see Cutler 1984; Simpson 1985). In the present experiment the flow in the boundary layer is parallel to the wall to within $\pm 5°$ so that the peak $-\overline{u_s v_s}$ is 14% lower than the peak $-\overline{uv}$

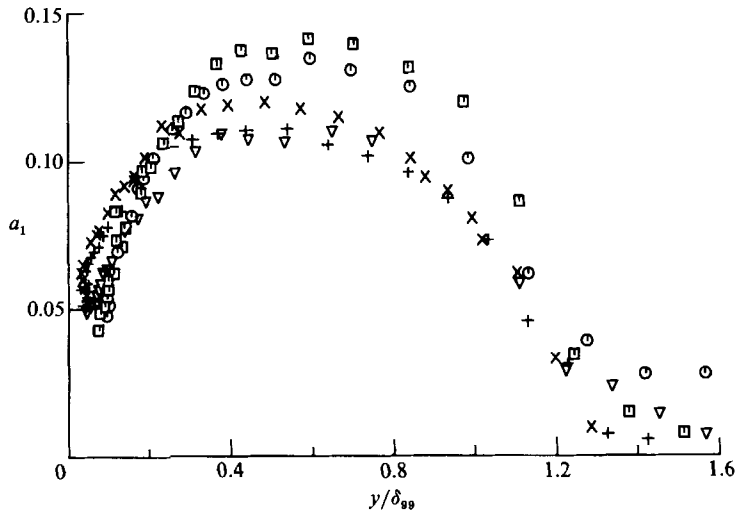

FIGURE 9. Profiles of the structural parameter a_1. For the profile locations, see figure 7.

at $x = 122$ mm, 6% lower at $x = 160$ mm and is not significantly different farther downstream. In comparing our data with model profiles for L, a_1, l, and ν_t, we have chosen to use streamline coordinates.

Since $\overline{w^2}$ was not measured in the experiment, we have followed the usual practice of assuming that $\overline{w^2} = \frac{1}{2}(\overline{u^2}+\overline{v^2})$ in calculating the turbulent kinetic energy ($\overline{q^2} = \overline{u^2}+\overline{v^2}+\overline{w^2}$). Shiloh, Shivaprasad & Simpson (1981) indicated that $\overline{w^2} = \overline{v^2}$ might be a better approximation in an adverse-pressure-gradient boundary layer near separation. If this assumption had been made then $\overline{q^2}$ would have been roughly 10% lower near the middle of the layer and roughly 20% lower near the wall. However, $\overline{w^2} = \overline{v^2}$ is a poor assumption near the wall where $\overline{v^2}/\overline{w^2}$ tends to zero, so that $\overline{q^2}$ is probably less than 10% too high. Profiles of the structural parameter, shown in figure 9, have been calculated using $\overline{w^2} = \frac{1}{2}(\overline{u^2}+\overline{v^2})$. The peak in a_1 falls to as low as 0.11, 25% below the generally accepted equilibrium value of 0.15, and rises only to about 0.12 at the most downstream station. The low values of a_1 may in part be attributable to the assumption made for $\overline{w^2}$.

Profiles of the eddy viscosity,

$$\nu_t = -\overline{u_s v_s} \Big/ \frac{\partial U}{\partial y},$$

are shown in figure 10. To be consistent, we should have used streamline coordinates in evaluating the mean velocity gradient but in the present case this makes practically no difference. Also shown in this figure is an outer-layer model due to Cebeci and Smith (see Cebeci & Bradshaw 1977), which is a fit to data from equilibrium turbulent boundary layers. The peak in the data profiles rises from about 0.03 close to reattachment to as high as 0.06 at $x = 199$ mm, before falling again to about 0.038 at $x = 465$ mm. This is still more than twice what the model predicts and the profiles at the last two stations indicate only a very slow approach to the model profile. Profiles of the mixing length,

$$l = (-\overline{u_s v_s})^{\frac{1}{2}} \Big/ \frac{\partial U}{\partial y},$$

are shown in figure 11. Also shown is the usual model for the wall region ($l = 0.41y$)

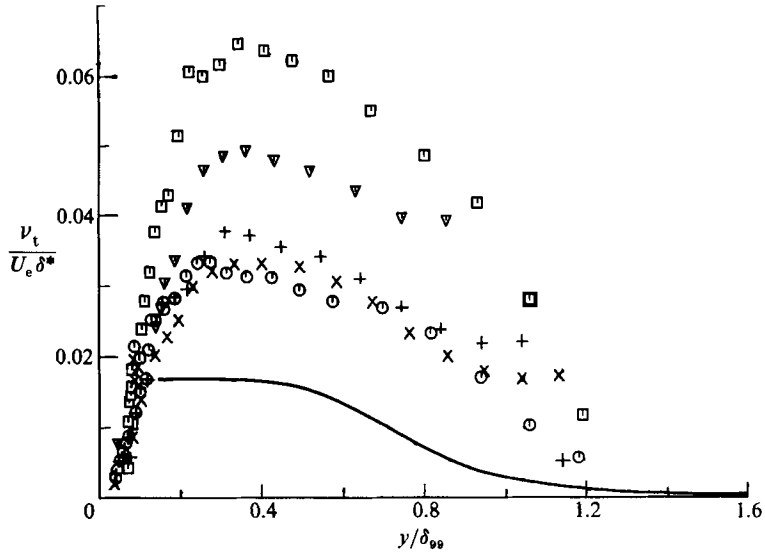

FIGURE 10. Profiles of the eddy viscosity and an equilibrium model due to Cebeci and Smith (——). For the profile locations, see figure 7.

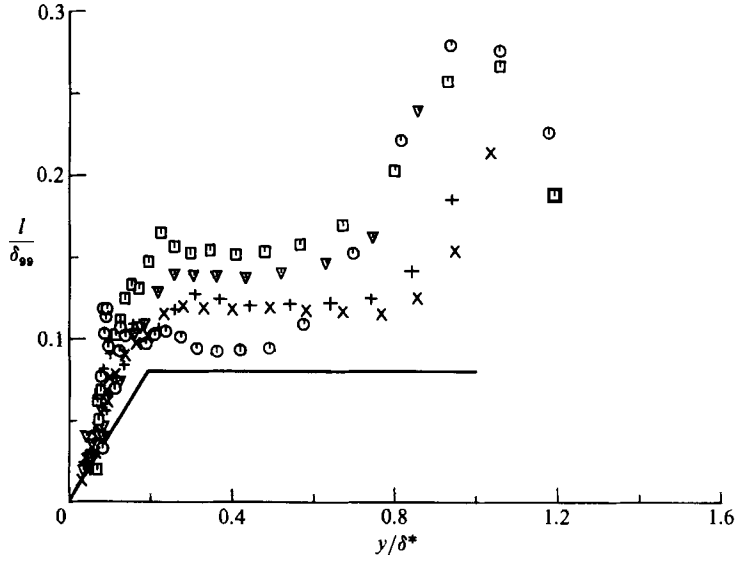

FIGURE 11. Profiles of the mixing length and an equilibrium model (——). For the profile locations, see figure 7.

and the standard outer-layer value (0.085). The behaviour of the mixing length is, not surprisingly, quite similar to the behaviour of the eddy viscosity so that the normalized mixing length near the centre of the layer rises rapidly after reattachment to a peak of about 0.16 at $x = 199$ mm before falling slowly to about 0.12 at $x = 618$ mm. In the wall region the data fall above $l = 0.41y$, but Galbraith & Head (1975) have demonstrated that this function (which works well in a zero pressure gradient) is not a good model in adverse-pressure-gradient boundary layers. It is likely that

any predictive method that assumes a unique relationship between mean velocity gradient and Reynolds shear stress in the outer layer will fail in this flow.

Although terms in the full momentum equations have not been derived from the data, terms in the integral momentum equation have been derived as part of the PL–PR check (see §2 and Cutler 1984). The contribution of the Reynolds normal-stress term is not negligible in comparison to other terms up to about $x = 400$ or 450 mm so that the Reynolds normal-stress terms should not be neglected in calculating flows close to reattachment.

The turbulent kinetic energy equation may be written for two-dimensional flows as follows:

$$\overbrace{\frac{\partial}{\partial x}U\frac{\overline{q^2}}{2}+\frac{\partial}{\partial y}V\frac{\overline{q^2}}{2}}^{\text{Convection}}+\overbrace{\frac{\partial}{\partial x}\overline{u\left(\frac{p'}{\rho}+\frac{q^2}{2}\right)}+\frac{\partial}{\partial y}\overline{v\left(\frac{p'}{\rho}+\frac{q^2}{2}\right)}}^{\text{Diffusion}}+\overbrace{\overline{uv}\frac{\partial U}{\partial y}+(\overline{u^2}-\overline{v^2})\frac{\partial U}{\partial x}}^{\text{Production}}+\overbrace{\epsilon}^{\text{Dissipation}}=0.$$

All the terms in this equation, except the fluctuating pressure contribution to the diffusion and the dissipation, have been evaluated directly using the measured profiles of mean velocity, Reynolds stresses and triple products. As before we assume that $\overline{w^2} = \frac{1}{2}(\overline{u^2}+\overline{v^2})$, and a similar assumption is made in estimating the triple product terms: $\overline{uw^2} = \frac{1}{2}(\overline{u^3}+\overline{uv^2})$ and $\overline{vw^2} = \frac{1}{2}(\overline{vu^2}+\overline{v^3})$. Direct numerical simulations and large-eddy simulations, for example the direct numerical simulation of a low-Reynolds-number turbulent channel flow by Moser & Moin (1984), suggest that the pressure diffusion term is small in comparison with the dissipation term (except possibly at reattachment). Profiles of dissipation were obtained by difference of the other terms in the turbulent kinetic energy equation (neglecting the pressure diffusion). The uncertainty in the dissipation evaluated in this way is inevitably very high, perhaps of the order of $\pm 30\%$.

The convection, diffusion, production and dissipation terms at $x = 160$ and 541 mm (non-dimensionalised with δ_{99} and U_e) are shown in figure 12. The terms are all larger in magnitude at the upstream station, where the turbulence levels are generally higher, than at the downstream station. The peak normal-stress production term ($(\overline{u^2}-\overline{v^2})\partial U/\partial x$) is 22% of the peak production at $x = 160$ mm and 10% at $x = 541$ mm, and the peak x-diffusion term ($\partial(\overline{uq^2})/\partial x$) is 33% of the peak diffusion at $x = 160$ mm and 21% at $x = 541$ mm. These terms are often neglected in boundary-layer calculation methods based on the turbulent kinetic energy equation, but they should be included for accurate calculation of flows near reattachment. Bradshaw (1967) presents an energy balance for an $a = -0.255$, $G = 14.5$ equilibrium adverse-pressure-gradient boundary layer for which the profile of the production term is similar in shape and magnitude to the production profile at $x = 541$ mm. Although the profiles of the other terms are also roughly similar in shape, the dissipation term in the present experiment is roughly twice that in Bradshaw's, the diffusion term is roughly the same, and the convection term is five or ten times larger. The relatively large magnitude of the convection term in the present flow is noteworthy.

The dissipation results are more easily interpreted by presenting them in the form of a lengthscale (figure 13):

$$L = (-\overline{u_s v_s})^{\frac{3}{2}}/\epsilon.$$

Our results are compared with the model of Bradshaw, Ferriss and Atwell (1967), which has been derived from zero and adverse-pressure-gradient equilibrium turbulent layer data and is similar to the models used for the mixing length. Indeed

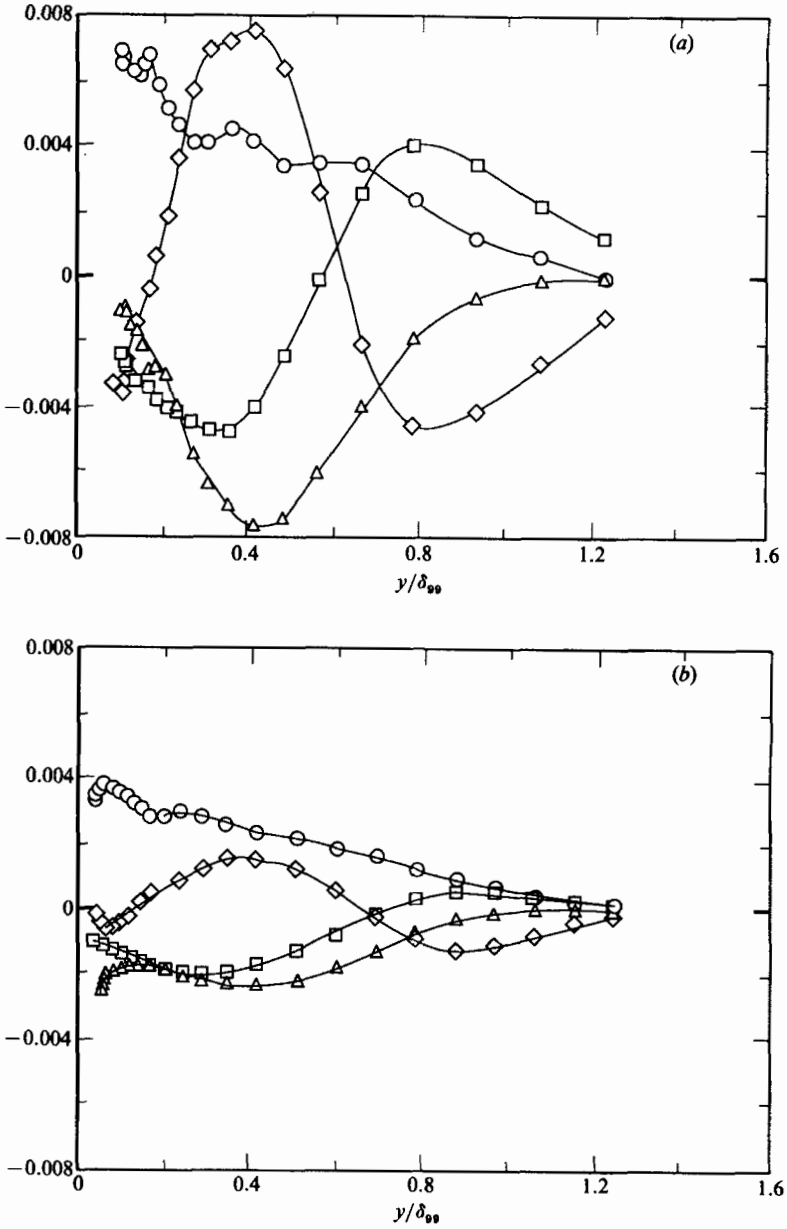

FIGURE 12. Profiles of terms in the turbulent kinetic energy equation at (*a*) $x = 160$ mm, (*b*) 541 mm; convection (□), production (△), diffusion (◇) and dissipation (○).

the mixing length and dissipation length are equal where the production of turbulent kinetic energy and the dissipation are equal, which is the case in the wall region of zero-pressure-gradient boundary layers and is often approximately the case in the outer layer. Our results show that the peak dissipation length at the upstream station is nearly three times larger than equilibrium – too great a difference to be accounted for by the large uncertainty in dissipation – but falls downstream so that by $x = 313$ mm it is close to equilibrium. The results do indicate a linear region close to the wall, but a little below the $L = 0.41y$ distribution implied by the model (a

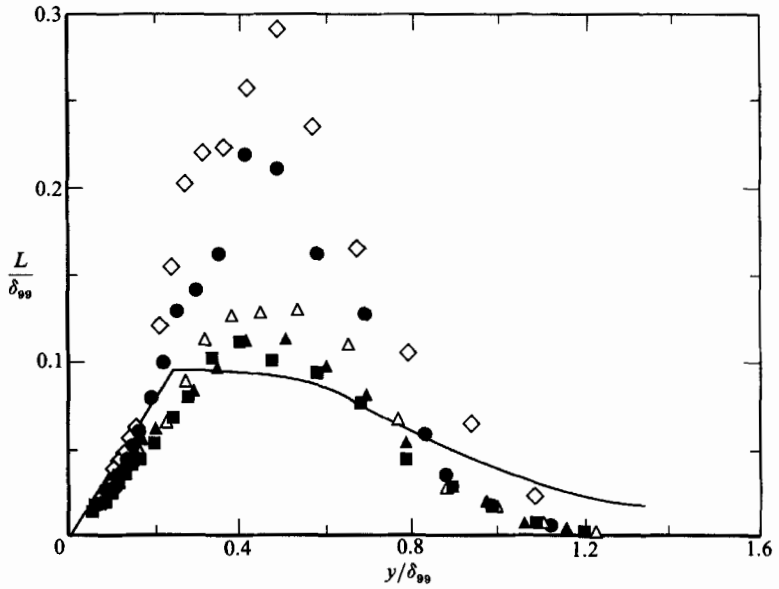

FIGURE 13. Profiles of the dissipation length and an equilibrium model due to Bradshaw *et al.* (1967) (——). The profiles are at $x = 160$ mm (◇), 237 mm (●), 313 mm (△), 389 mm (■) and 541 mm (▲).

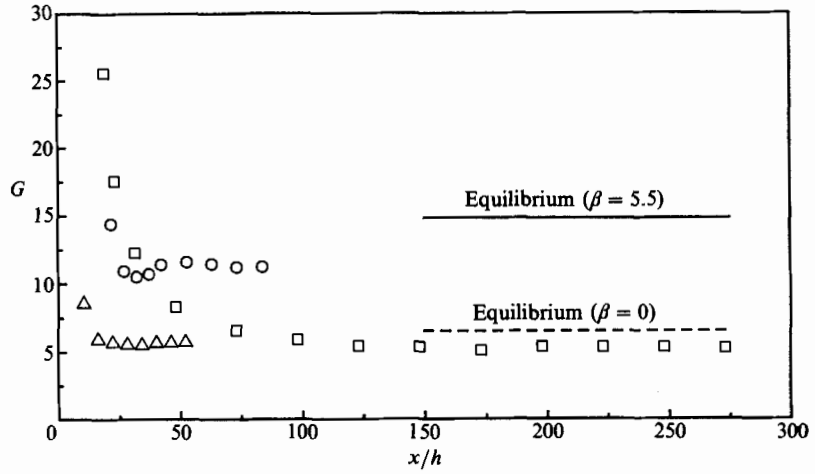

FIGURE 14. Comparison of the development of G for the present case (○) with the development for reattached boundary layers in zero pressure gradient; the Tillman 'ledge' flow (Coles & Hirst 1968) (□); and a backstep flow (Bradshaw & Wong 1972) (△).

discrepancy possibly attributable to experimental uncertainty). Another, more recent, model for the dissipation length in a boundary layer, which apples to a wide range of turbulent, wall-bounded shear flows, is described by Hunt, Spalart & Mansour (1987); it may be written in the following form:

$$L = \left(-\frac{\overline{uv}}{\overline{v^2}}\right)^{\frac{3}{2}} \left(\frac{A_B}{y} + A_S \frac{\partial U}{\partial y} \Big/ \overline{v^2}^{\frac{1}{2}}\right)^{-1},$$

where $A_B = 0.27$ and $A_S = 0.46$. The dissipation length has been evaluated from our

measurements using this model and compared to the directly evaluated dissipation length and Bradshaw's model. The agreement is excellent at the downstream station ($x = 541$ mm) but, although the model does predict a rise in dissipation length scale after reattachment (to a peak of about $L/\delta_{99} = 0.17$ at $x = 160$ mm), the rise is underpredicted. Hunt's model agrees well with the $L = 0.41y$ distribution in the wall region.

5. Discussion

The results seem to indicate two distinct regions of development. (i) An upstream region, from reattachment to $x = 400$ or 450 mm ($54h$ or $61h$), in which the flow changes rapidly as it adjusts to the new boundary condition. In this region the Clauser parameter G falls rapidly and the eddy viscosity first rises rapidly to four times normal values then falls more slowly. (ii) A region downstream of this in which G and β are both nearly constant and profiles of eddy viscosity are nearly self-similar. In this region the boundary layer would appear to be near to equilibrium, except that the eddy-viscosity coefficient is twice as large as is expected, and G is significantly lower (given β) on the basis of previous studies of equilibrium boundary layers. Unlike eddy viscosity and mixing length (which relate the shear stress to the velocity gradient), those parameters which relate turbulence quantities to one another (i.e. a_1 and L) have distributions fairly close to equilibrium in the downstream region.

A comparison with the development of G for the present case with the development in the zero-pressure-gradient flows downstream of a square-section fence (see the Tillman 'ledge' flow in Coles & Hirst 1968) and downstream of a backward-facing step (Bradshaw & Wong 1972) is shown in figure 14. All three flows have a region in which G falls rapidly, undershooting the equilibrium value calculated using the correlation of Nash (1965), followed by a region in which it is nearly constant or (in the zero-pressure-gradient cases) in which it appears to rise slowly towards equilibrium. In no case does G reach normal equilibrium values by the last measurement station, and the slow rate of change in the streamwise distance suggests that it will not do so for a considerable distance (several hundred fence heights for the fence flows).

Although there are qualitative similarities in the development of G for the flows shown in figure 14, there are large differences in the x-distance to the point of minimum G, and the minimum value of G itself. However these may be explained by the differences in the geometries upstream of reattachment and differences in the pressure gradient. The fence geometry and Re_h for the present case and the Tillman flow are similar, but Bradshaw & Wong (1972) have shown that the much larger upstream boundary-layer thickness ($\delta_{99} = 3.3h$) in the Tillman case results in the larger distance (in terms of step heights) from reattachment to the point of minimum G. The differences between fence flows and backstep flows are much greater: (i) fence flows typically have a much longer reattachment length than backstep flows, which may be attributed to the initial deflection of the mean streamlines away from the wall by the fence (the reattachment lengths are $x_r = 13.5h$ for Tillman's ledge flow, $x_r = 15.6 \pm 0.7h$ for the present fence flow, and $x_r = 6h$ for Bradshaw's flow); (ii) the Reynolds stresses in the free shear layer and at reattachment are typically up to twice those in backstep flows, probably as a result of higher reversed-flow velocities and so greater velocity differences across the shear layer. As a result, the fence flows require a greater distance (in terms of step heights) to reach the minimum G point and, farther downstream, to reach equilibrium.

A comparison with the more detailed investigations of reattachment downstream of a backward-facing step and the relaxation in a parallel duct by Kim, Kline and Johnston (1980) ($x_r = 7 \pm 1h$), and by Driver & Seegmiller (1985) ($x_r = \pm 6.1h$) have revealed further similarities to the present flow in the upstream region. Kim *et al.* observed a rapid rise in mixing length and eddy viscosity (non-dimensionalized in the normal manner) downstream of reattachment. Peak values of eddy viscosity ($\nu_t/(U_e \delta^*)$) as high as 0.085 and outer-layer values of mixing length (l/δ_{99}) as high as 0.2 were observed at $x = 15.7h$, higher even than in the present flow. Driver & Seegmiller obtained profiles of terms of the turbulent kinetic energy equation using similar assumptions for the terms containing w and the pressure diffusion to the ones we have made. These results indicate dissipation lengths (L/δ_{99}) of about 0.1 at $x = 8h$ and 0.2 at $x = 12h$, which are above the equilibrium levels proposed by Bradshaw *et al.* (1967), although possibly not significantly so given the high uncertainty in the dissipation measurement. These more detailed investigations do not go far enough downstream to observe the region seen in the present flow (discussed above), where G and profiles of eddy viscosity coefficient change slowly.

The present results are consistent with the three-layer structure of reattached boundary layers proposed by Bradshaw & Wong (1972), which consists of (i) 'a local-equilibrium layer, following the logarithmic law, which spreads out from the wall'; (ii) 'a layer in which... the dissipation length parameter, increases above the local equilibrium value with increasing y' (see figure 13); and (iii) 'an outer layer which, except for the effects of rapid distortion near reattachment, will retain the characteristics of the mixing layer until the effects of the altered boundary condition at the surface propagate through it'. In Bradshaw's experiment and most other reattached-boundary-layer studies (in zero pressure gradient) the junction of layers (i) and (ii) is visible as a marked dip in the mean velocity profiles below the logarithmic law. However, the absence of such a dip in our experiment can be explained by consideration of the relative magnitude of the terms in the turbulent kinetic energy equation:

$$\frac{\partial U}{\partial y} = \frac{(-\overline{uv})^{\frac{1}{2}}}{L} + \frac{\text{convection} + \text{diffusion}}{-\overline{uv}}.$$

In most zero-pressure-gradient boundary layers, convection and diffusion may be neglected close to the wall and the turbulent shear stress is approximately constant (except in the laminar sublayer). If we assume also that $L = 0.41y$ the above equation may be integrated to give the logarithmic law and any increase in L above $0.41y$ will cause the mean velocity to dip below the logarithmic law. However, where the pressure gradient is adverse the convection and diffusion terms are comparable in size with the production term near the wall and of the same sign (negative). Also, the shear stress is no longer constant with respect to y but is rising. The result is that, although our data indicate a rise in L above $0.41y$, the behaviour of the dissipation term is less important in determining the mean velocity profile and there is no dip below the logarithmic law.

The great sensitivity of the boundary-layer structure to the perturbation, even far downstream, is interesting and is in general agreement with the results of previous studies. The effects of body forces or extra rates of strain (equivalently, the effect of extra production terms on the Reynolds stress transport equations) are known to be surprisingly large (Bradshaw 1975). For example, the effects of streamwise curvature, lateral divergence, bulk dilatation, and buoyancy forces are as much as an order of

magnitude greater than expected from the size of the explicitly extra generation terms. Thus, local-equilibrium (eddy viscosity or mixing length) types of model generally prove inaccurate. Whilst the extra $(\partial U/\partial x)$ production terms in equilibrium adverse-pressure-gradient boundary layers are not normally large enough to have a significant effect, the unusual magnitude of some of the terms in the transport equations for the reattached layer apparently are. Hunt, Stretch & Britter (1988) have attributed the high sensitivity of turbulent boundary layers to buoyancy effects to a dependence of the dissipation lengthscale on the shear $(\partial U/\partial y)$. If the turbulent kinetic energy equation is cast in the form

$$-\overline{uv}\frac{\partial U}{\partial y} - P_e = \epsilon,$$

were P_e are the extra production terms, and the convection and diffusion terms, then using Hunt's equation for the dissipation length we obtain the following expression for the mixing length:

$$\frac{l}{l_0} = \left(1 + \frac{P_e y}{A_B(\overline{v^2})^{\frac{3}{2}}}\right)^{-1};$$

where l_0 is the distribution when P_e is small. However, if Bradshaw's model, which is of the form $L/\delta_{99} = F(y/\delta_{99})$, is used then the expression is

$$\frac{l}{l_0} = \left(1 + \frac{P_e \delta_{99} F}{(-\overline{uv})^{\frac{3}{2}}}\right)^{-1}.$$

The term that multiples P_e is at least four times greater in a typical boundary layer if Hunt's model is used, indeed suggesting a much higher than expected sensitivity of turbulent boundary layers to perturbation in general.

6. Conclusions

The relaxation of a reattached turbulent boundary layer downstream of a wall fence has been investigated. The boundary layer has an adverse pressure gradient imposed upon it which is adjusted in an attempt to bring the boundary layer into equilibrium. This is done by adjusting the pressure gradient so as to bring the Clauser parameter (G) to a value of about 11.4 and then maintain it roughly constant. Detailed measurements with hot-wire anemometers in the region from reattachment to $x = 83h$ are presented.

(i) Two regions of the flow have been identified. In the upstream region (from reattachment to $x = 54h$ or $61h$) G falls rapidly to about 11.4 and the eddy viscosity and mixing length profiles (non-dimensionalized in the conventional way) rise rapidly and then fall again more slowly. In the downstream region, G and the pressure gradient parameter (β) are roughly constant (as one would expect if the boundary layer were equilibrium), and profiles of the mixing length and eddy viscosity coefficient are roughly self-similar. However both β and eddy viscosity are about twice as large as expected on the basis of previous studies of equilibrium boundary layers (given G).

(ii) Qualitatively similar results are observed in zero-pressure-gradient boundary layers downstream of reattachment, although there is no single, detailed, experiment that goes sufficiently far downstream to make quantitative comparisons. The layered structure observed in profiles of mean velocity in a zero pressure gradient is absent in the present case because, in part, of the greater convection and diffusion of

turbulent kinetic energy from near the middle of the boundary layer towards the wall (relative to the local production) in adverse-pressure-gradient boundary layers.

(iii) It is not clear from the results of this experiment (or from the literature) whether, if we had made measurements sufficiently far downstream, we would have seen the development of a 'normal', equilibrium, adverse-pressure-gradient boundary layer. It is clear however that such a layer will only be reached after several hundred step heights of streamwise development.

(iv) Within the upstream region mentioned above many of the terms usually neglected in simplifying the momentum and turbulent kinetic energy equations for boundary-layer calculations should not be neglected. Specifically, the $\partial(\overline{u^2}-\overline{v^2})/\partial x$ term in the x-component momentum equation, and the $(\overline{u^2}-\overline{v^2})\,\partial U/\partial x$ and $\partial(\overline{uq^2})/\partial x$ terms in the turbulent kinetic energy equation are not small. The use of a streamline coordinate system in this region may be of some use in the modelling of quantities containing the turbulent shear stress.

The work presented here was accomplished at Stanford University with substantial support from the Dept of Mechanical Engineering, the Office of the Dean of Graduate Studies and Research, and the Industrial Affiliates of the Thermosciences Division. The authors would like to acknowledge the helpful comments of Professor Peter Bradshaw of Imperial College and of the Journal referees.

REFERENCES

BARLOW, R. S. & JOHNSTON, J. P. 1985 Roll-cell structure in a concave turbulent boundary layer. *AIAA*-85-0297.

BRADSHAW, P. 1967 The structure of equilibrium boundary layers. *J. Fluid Mech.* **29**, 625–645.

BRADSHAW, P. 1971 *An Introduction to Turbulence and Its Measurement.* Pergamon.

BRADSHAW, P. 1975 Review – complex turbulent flows. *Trans. ASME* I: *J. Fluids Engng* **97**, 146–154.

BRADSHAW, P., FERRISS, D. H. & ATWELL, N. P. 1967 Calculation of boundary layer development using the turbulent energy equation. *J. Fluid Mech.* **28**, 593–616.

BRADSHAW, P. & WONG, F. Y. 1972 The reattachment and relaxation of a turbulent shear layer. *J. Fluid Mech.* **52**, 113–135.

BREDERODE, V. DE & BRADSHAW, P. 1978 Influence of side walls on the turbulent center-plane boundary-layer in a square duct. *Trans. ASME* I: *J. Fluids Engng* **100**, 91–96.

CASTRO, I. P. 1981 Measurements in shear layers separating from surface mounted bluff bodies. *J. Wind Engng Ind. Aero.* **7**, 253–272.

CASTRO, I. P. & FACKRELL, J. E. 1978 A note on two-dimensional fence flows, with emphasis on wall constraint. *J. Ind. Aero.* **3**, 1–20.

CEBECI, T. & BRADSHAW, P. 1977 *Momentum Transfer in Boundary Layers.* Hemisphere.

CLAUSER, F. H. 1954 Turbulent boundary layers in adverse pressure gradients. *J. Aeronaut. Sci.* **21**, 91–108.

CLAUSER, F. H. 1956 The turbulent boundary layer. *Adv. Appl. Mech.* **4**, 1–51.

COLES, D. E. & HIRST, E. A. (eds.) 1968 *Proceedings, Computation of Turbulent Boundary Layers* – 1968 *AFOSR-IFP-Stanford Conference*, vol II. Dept. of Mech. Engng, Stanford University.

CUTLER, A. D. 1984 Adverse pressure gradient and separating turbulent boundary layer flows: the effect of disequilibrium in initial conditions. Ph.D. Thesis (also Rep. MD-31), Dept of Mech. Engng, Stanford University, available from University Microfilms.

DRIVER, D. M. & SEEGMILLER, H. L. 1985 Features of a reattaching shear layer in a divergent channel flow. *AIAA J.* **23**, 163–171.

EAST, L. F. 1981 A representation of second-order boundary layer effects in the momentum integral equation and in viscous–inviscid interactions. *RAE Tech. Rep.* 81002.

EAST, L. F. & SAWYER, W. G. 1979 An investigation of the structure of equilibrium turbulent boundary layers. *Turbulent Boundary Layers: Experiment, Theory and Modeling, AGARD CP-271.*

GALBRAITH, R. A. McD. & HEAD, M. R. 1975 Eddy viscosity and mixing length from measured boundary layer developments. *Aero. Q.* **26**, 133–154.

HUNT, J. C. R., SPALART, P. R. & MANSOUR, N. N. 1987 A general form for the dissipation length scale in turbulent shear flows. *Center For Turbulence Research, Proc. Summer Program 1987.*

HUNT, J. C. R., STRETCH, D. D. & BRITTER, R. E. 1988 Length scales in stably stratified turbulent flows and their use in turbulence models, *Proc. IMA Conference on Stably Stratified Flows and Dense Gas Dispersion, Chester, April 9–10.*

HUSSAIN, A. K. M. F. & REYNOLDS, W. C. 1975 Measurements in a fully developed turbulent channel flow. *Trans. ASME* I: *J. Fluids Engng* **97**, 568–580.

KIM, J., KLINE, S. J. & JOHNSTON, J. P. 1980 Investigation of a reattaching turbulent shear layer: flow over a backward facing step. *Trans. ASME* I: *J. Fluids Engng* **102**, 302–308.

MOSER, R. D. & MOIN, P. 1984 Direct numerical simulation of curved turbulent channel flow. *Rep.* TF-20. Dept. of Mech. Engng, Stanford University.

NASH, J. F. 1965 Turbulent-boundary-layer behaviour and the auxiliary equation. In *AGARDograph* 97, Part 1, pp. 245–249.

SHILOH, K., SHIVAPRASAD, B. G. & SIMPSON, R. L. 1981 The structure of a separating turbulent boundary layer. Part 3. The transverse velocity measurements. *J. Fluid Mech.* **113**, 75–90.

SIMPSON, R. L. 1985 Two-dimensional separated flow. *AGARDograph* 287, Vol. 1.

SMITS, A. J. & WOOD, D. H. 1985 The response of turbulent boundary layers to sudden perturbations. *Ann. Rev. Fluid Mech.* **17**, 321-358.

TOWNSEND, A. A. 1960 Equilibrium layers and wall turbulence. *J. Fluid Mech.* **11**, 97–120.

TOWNSEND, A. A. 1976 *The Structure of Turbulent Shear Flow* (2nd edn.). Cambridge University Press.

WESTPHAL, R. V. & JOHNSTON, J. P., 1983 Experimental study of flow reattachment in a single-sided sudden expansion. *Rep. PD-41, Dept. of Mech. Engng, Stanford University.*

WHITE, F. M. 1974 *Viscous Fluid Flow.* McGraw-Hill.